Coherent crystallography of shear-aligned crystals of hard-sphere colloids

J. Liu
Department of Physics, California State University at Long Beach, Long Beach, California 90840

D. A. Weitz
Exxon Research and Engineering Co., Route 22E, Annandale, New Jersey 08801

B. J. Ackerson
Department of Physics, Oklahama State University, Stillwater, Oklahoma 74078

(Received 1 April 1993)

The structure of colloidal crystals formed from suspensions of hard-sphere colloids is studied. The samples are contained in a thin cell. By rocking the samples, we are able to form shear-aligned colloidal crystals with extended, long-range order. The aligned crystals persist after the shear ceases, enabling us to use laser-light crystallography to determine their structure. We observe an unusual ordering, wherein the structure is a nearly perfect single twin of a face-centered cubic crystal, with crystals of different twins formed on each side of the cell. We exploit the coherence of the laser source to observe a speckle-like fluctuation of the intensity in the Bragg peaks. However, this fluctuation occurs only in one scattering direction, and therefore reflects a remnant disorder in the stacking of the hcp planes. We introduce a simple model which accounts for both the nature of the disorder in the stacking as well as the specklelike fluctuations. Our observation of this speckle also confirms recent predictions.

PACS number(s): 61.50.Ks, 81.40.−z, 82.70.Dd

INTRODUCTION

Suspensions of uniformly sized colloidal particles interacting solely through excluded volume, or hard-sphere colloids, form one of the simplest, yet most important models for the study of the physical properties of concentrated suspensions. For example, they exhibit a very rich phase behavior as the volume fraction of solids, ϕ, is varied [1,2]. At low ϕ, the particles exhibit a random, liquidlike, disordered structure. As the volume fraction is increased above $\phi \sim 0.494$, an ordered crystalline phase can coexist with the disordered liquid phase. These coexisting phases persist until $\phi \sim 0.545$, whereupon only the crystalline phase exists in equilibrium. Finally, when the volume fraction increases above $\phi \sim 0.58$, packing constraints of the particles apparently preclude the formation of structures with long-range crystalline order, and a glassy structure is observed instead. The rheological properties of hard-sphere suspensions also possess a very rich and complex behavior [3–7] exhibiting both shear thinning and shear thickening, depending on the shear rate and volume fractions. This behavior has been extensively studied and has been shown to be correlated with the structures induced in the colloidal suspensions by the shear [3,4,7]. At low shear rates, the shear tends to induce crystalline order in the particles, making it easier for them to flow over one another, and thus resulting in shear thinning. At higher shear rates, this order is destroyed, making the flow of the particles more difficult, and therefore resulting in shear thickening [3,4].

The relationship between the rheological behavior and the structure of the particles has been extensively studied [8]. It is also possible to exploit this behavior to use shear to induce order in suspensions of hard-sphere colloids [6,7,9]. For example, steady shear can induce crystal-like order in hard-sphere suspensions whereby hexagonally close-packed (hcp) layers are aligned perpendicular to the shear direction, with close-packed lines of particles along the velocity direction. The hcp layers can be stacked either in a face-centered-cubic (fcc) lattice or in a random stacking of hcp and fcc order. Oscillatory shear can also produce an ordered fcc structure, but with close-packed lines of atoms oriented perpendicular to the velocity direction. Other ordered structures are also produced, depending on whether the shear is steady or oscillatory, and depending on the strain amplitudes applied. However, in all cases reported to date, the crystal structure relaxes and the ordering is destroyed after the application of the shear has ceased.

Producing shear-aligned suspensions which retain their order would be of great potential technological use: Suspensions with extended ordered regions may serve as high-quality precursors for ceramic materials [10]. Moreover, these aligned colloidal crystals would make ideal systems for the study of the physical properties of ordered colloidal suspensions. For example, it may be possible to use these shear-aligned colloidal crystals to study the consequences of a reduction in the phase space available for optical transitions within the crystal [11]. In addition, since the size of the colloidal particles, and their spacing, can be on the order of the wavelength of light, crystallography of these samples can be studied with a laser, with its inherent coherence. This presents an ideal system for an experimental test of recent theoretical predictions of specklelike patterns in diffraction spots of ordered structures [12]. This is of particular current

relevance because advances in synchrotron brightness are just now providing x-ray sources with appreciable spatial coherence, and speckle has recently been observed in the Bragg peaks of an atomic crystal [13]. Thus the use of laser crystallography to study colloidal crystals presents an opportunity to explore the additional information crystallography with a coherent source can provide. For all these purposes, knowledge and control of the structure of the shear-aligned colloidal crystals is essential.

In this paper, we study the structure of shear-aligned crystals formed from hard-sphere colloids. We use a suspension with a volume fraction of $\phi \sim 0.56$, where the equilibrium phase is completely crystalline. Equilibrium nucleation and growth of the crystals results in the formation of a polycrystalline order, with crystallites of size of order 10–50 μm. By applying shear in a very simple geometry, we are able to align the sample and form crystals with extended order. We determine the structure of these crystals through the use of laser-light crystallography. The structure most often obtained is quite different from that obtained in crystals formed by equilibrium nucleation and growth, where a random stacking of hexagonally close-packed (hcp) planes is usually observed [14]. Instead, we observe a strong predominance of face-centered-cubic crystals over a large portion of the sample, as evidenced by three sharp Bragg peaks. Surprisingly, these fcc crystals consist almost exclusively of a single twin. Moreover, different twins are formed on either side of the cell and the volume fraction of the crystalline region is increased substantially. This makes the crystals quite stable, allowing us to store them for many weeks. While the crystals have extended positional order of the spheres in three dimensions, they nevertheless still have some randomness in the stacking of the planes, leading to a distinct form of disorder in the crystal structure. To explore the nature of this disorder, we exploit the coherence of the laser source, and observe a form of speckle pattern within the Bragg peaks themselves. The existence of these speckles has recently been predicted theoretically [12] for crystals exhibiting this form of disorder, but has, to date, not been observed experimentally in atomic crystals with similar structures due to the limited coherence of x-ray sources. Finally, in some regions, we also observe a structure with a sixfold symmetry, corresponding to a random stacking of hcp planes, as is observed for crystals formed by equilibrium nucleation. We are again able to determine the extent of the order in this structure using the speckle patterns observed within the Bragg peaks.

BRAGG SCATTERING

The colloids used in this study are monodisperse polymethylmethacrylate (PMMA) spheres, with a diameter of 0.68 μm. They are sterically stabilized by a thin layer of grafted polymer about 15 nm thick. This ensures that the particles interact with each other solely through hard-sphere repulsion [2,15]. The colloids are suspended in a mixture of dodecane and carbon disulfide to match the index of refraction of the particles to that of the suspending fluid, thereby avoiding the problems of multiple scattering of light and enabling us to use laser-light crystallography to study the crystal structures. The initial volume fraction of the colloids is chosen to be about $\phi \sim 0.56$, to ensure that the equilibrium phase is purely crystalline [2]. The sample is sealed in a thin, 1-mm-thick rectangular cuvette. Shear is applied to the sample by rocking the cell about an axis parallel to its thinnest dimension. This results in macroscopic flow of the suspension at the top of the cell as it moves from side to side. The induced velocity fields in the cell are shown schematically in Fig. 1. The dominant shear results from the Poiseuille flow of the sample across the thinnest dimension of the cuvette, as shown in Fig. 1.

The samples are initially tumbled and are thus in a

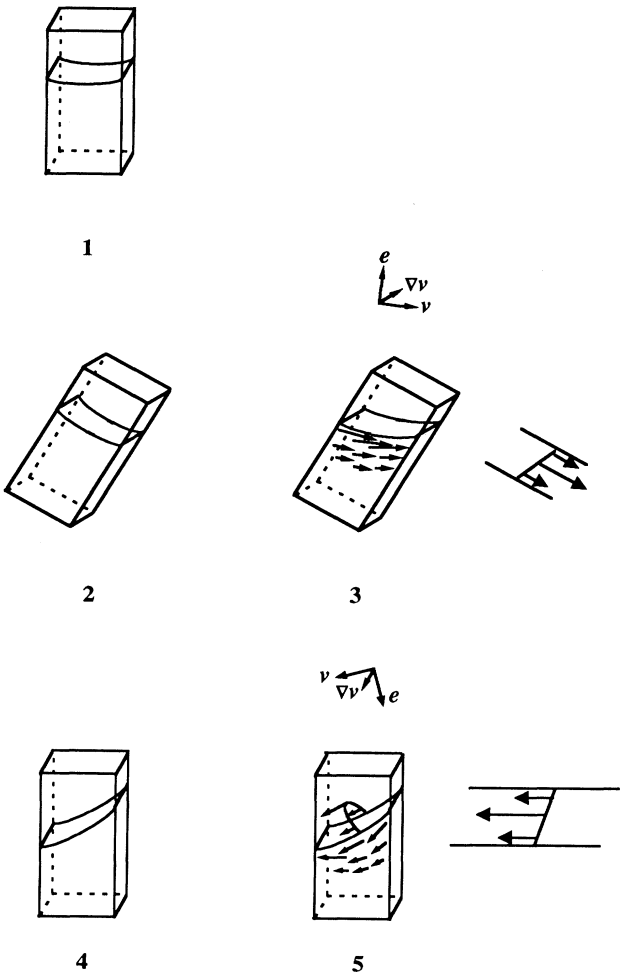

FIG. 1. Schematic view of the flow patterns which cause the shear alignment as the cell is rocked. The arrows point in the direction of the flow, and their length indicates the local velocity. The arrows in the cell are meant to indicate the variation of the average velocity over the face of the cell. The variation of the velocity across the thin dimension of the cell is determined by the Poiseuille flow, and is indicated by the figures to the right of diagrams 3 and 5. The small set of indices above the cell in diagrams 3 and 5 indicate directions of the velocity v, shear Δv, and vorticity e, at the front surface of the cell during that portion of the rocking motion.

disordered state. If they are allowed to equilibrate for about an hour, small randomly oriented crystallites begin to nucleate. The application of shear by rocking the cell effectively realigns the sample to form colloidal crystals with long-range order. We estimate that the maximum shear rate at the top of the cell is about 10 sec^{-1}. However, the shear rate is not uniform over the whole cell, but decreases towards the bottom as the amount of macroscopic flow of the suspension is reduced. This is illustrated schematically by the arrows in Fig. 1. With this simple method, we are able to form shear-aligned colloidal crystals that are well ordered over extended areas. Once formed, we find that the shear-aligned structures can be stable for many weeks. All our scattering studies are performed after the shear is stopped.

We use laser-light crystallography to determine the structure of the colloidal crystals formed after the shear. The laser beam is incident on the cell parallel to the thinnest axis, and the Bragg scattering of the transmitted light is observed on a screen placed about 10 cm from the sample. We use several laser lines from both Ar^+ and Kr^+ lasers as sources, enabling us to easily vary the laser wavelength, and hence the scattering wave vector. The sample is translated in the beam to allow different positions in the cell to be studied. Because of the variation of the scattering form factor of the spheres, and the effects of the geometry, rotation of the sample cell to vary the scattering wave vector, and the orientation of the scattering vector with respect to the orientation of the colloidal crystal, proved to be impracticable.

Before the application of shear, the equilibrium state of the colloid is comprised of small, randomly oriented crystallites. The diffraction pattern of this sample consists of an extended ring of Bragg spots. Rocking the sample several times is sufficient to shear-align the crystals, producing extended, long-range order in the sample, as evidenced by the diffraction pattern, which exhibits six sharp spots, as illustrated in Fig. 2. This pattern is obtained from a region near the bottom of cell, using the 514.5-nm laser line of the Ar^+ laser. The existence of only six sharp spots implies that the shear has aligned the crystal, and it now possesses long-range positional order. The sixfold symmetry is consistent with the formation of hexagonally close-packed planes aligned parallel to the flat surface of the cell. This form of ordering is often observed in sheared suspensions of hard-sphere colloids while the shear is applied [3,4,6,7] but has not been reported to persist after cessation of the shear. The shear-induced stresses force lines of close-packed colloids to form along the velocity direction, and these lines are packed into registered hexagonally close-packed planes by the constraints of the volume fraction. Consistent with this interpretation, we find that the orientation of the six spots rotates as the beam is scanned horizontally across the cell, mimicking the velocity profile.

Despite the observation of six sharp diffraction spots, the shear-aligned structure cannot have perfect long-range crystalline order. Since the hcp planes are aligned parallel to the flat surface of the cell by the shear, and since the light is incident normal to this face, the angle of incidence is defined relative to these planes. Moreover,

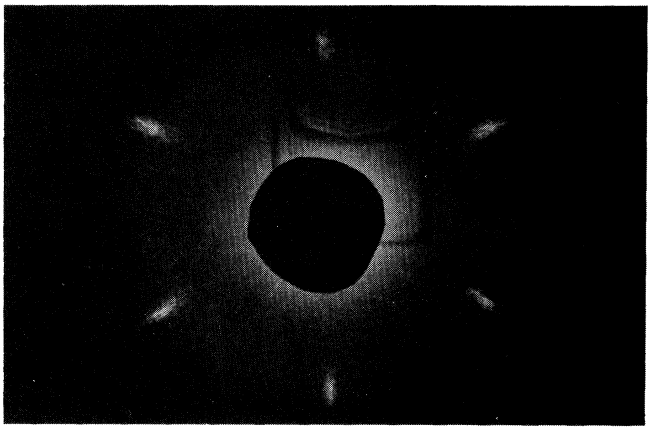

FIG. 2. Diffraction pattern of a shear-aligned colloidal crystal, showing six sharp Bragg peaks. The laser beam is incident near the bottom of the cell.

the size of the spheres, and their volume fraction, determine the spacing between the hcp layers. Thus, for a perfect crystal, the Bragg condition can be satisfied only for a specific wavelength of light, λ. It is unlikely that we have arbitrarily met the Bragg condition with the laser line used. To ascertain this, we measure the diffraction pattern with other laser lines. We find a similar sixfold symmetric pattern with all laser lines used from 647.1 to 413.1 nm, with the scattering angle decreasing as the wavelength decreases. Thus the structure is not a perfect crystal. Instead, the observed diffraction pattern is most likely caused by a random stacking of hcp planes.

To describe the diffraction pattern, we consider the packing of registered hcp planes of spheres. If the first hcp plane of spheres near the wall is denoted by A, there are two possible orientations for the next plane, either B, obtained by a translation of $\mathbf{a}/3+2\mathbf{b}/3$ relative to A, or C, obtained by a translation of $2\mathbf{a}/3+\mathbf{b}/3$ relative to A. Here $\mathbf{a}$ and $\mathbf{b}$ are hexagonal lattice vectors in the plane while $\mathbf{c}$ is the lattice vector perpendicular to the plane, in the stacking direction. A perfect fcc crystal would consist of an $ABCABC$ stacking sequence, or its twin, $ACBACB$, while a perfect hcp crystal would consist of an $ABABAB$ or $ACACAC$ stacking sequence. In reciprocal space, a single layer of hexagonally packed spheres results in rods of intensity in the l direction, parallel to the $\mathbf{c}$ direction in real space. These rods are situated in a hexagonal pattern around the origin, a distance $2\pi/d_h$ away from the origin, along q_h or q_k, where $d_h=\sqrt{3}d/2$, and d is the diameter of the spheres, and where $\mathbf{h}$ and $\mathbf{k}$ are rotated 30° from $\mathbf{a}$ and $\mathbf{b}$, respectively. They occur at $\{hkl\}=\{10l\}$, $\{01l\}$, $\{11l\}$, $\{\bar{1}0l\}$, $\{0\bar{1}l\}$, and $\{\bar{1}\,\bar{1}l\}$, where distance is measured in units of $2\pi/d_h$ along the $\mathbf{h}$ and $\mathbf{k}$ directions. A perfect hcp crystal results in a hcp lattice in reciprocal space, comprised of lattice points rather than intensity rods. These lattice points are also sixfold symmetric, and occur every $n\pi/d_l$ along q_l, where n is an integer and d_l is the spacing between two layers. By contrast, a single twin of a fcc crystal results in a threefold symmetric pattern in reciprocal space, as it consists of Bragg spots every $2\pi/d_l$ but the spots are

offset by $\pi/3d_l$ along three of the rods with respect to the other three. Thus, along three of the rods, the spots occur at $q_l=\pi/3d_l$, while along the other three, they occur at $q_l=2\pi/3d_l$. For the other fcc twin, the first set of $\{hkl\}$ rods have the Bragg spots at $q_l=2\pi/3d_l$, while the second set have them at $q_l=\pi/3d_l$. In all cases, Bragg spots would be observed only with selected wavelengths, that match the well-defined lattice points. By contrast, a random packing of hcp layers results in Bragg scattering with all wavelengths. In this case, the reciprocal lattice is not made up of isolated lattice points, but instead the lattice points are broadened into rods of intensity along q_l [16–18]. Thus the position of the rods is determined by the spacing of the spheres in the planes, while the intensity along the rods is determined by the actual packing sequence. For example, for a completely random sequence, the intensity along the rods varies by a factor of 9 as the scattering wave vector along the rods, q_l, varies by π/d_l. The structure along each of the rods is the same, so that the diffraction pattern is sixfold symmetric. This structure accounts for our observation of six sharp spots for all laser lines. This form of crystal structure is frequently observed for hard-sphere colloids, both when they are formed spontaneously as ϕ is increased and when they are aligned by steady shear.

From the diffraction pattern, it should, in principle, be possible to determine the spacing between the spheres. However, a complete determination would require full knowledge of the diffraction pattern, and in particular, would require a scan of the scattered intensity along q_l in order to determine the spacing between the layers. Unfortunately, this is very difficult to do because of the effects of the form factor of the spheres. We are instead able to obtain some information about the intensity along q_l by changing the scattering wave vector by using different laser lines. Here again it is not possible to make accurate measurements of the relative scattered intensity as the wavelength is changed. We can, however, accurately determine the scattering vector in the plane parallel to the flat face of the cell. This enables us to determine the spacing of the spheres within the plane, and since they are packed on a hexagonal lattice, this should also determine all the spacings, provided that the spacing between spheres of adjacent planes is the same as that between spheres within a plane. We determine the scattering wave vector within the hk plane by measuring the scattering angle and correcting for the refraction at the interfaces and the index of refraction inside the sample. From this, we calculate the spacing between the spheres in the plane. Surprisingly, we find that the spheres are separated by 685 ± 10 nm, which, to within the accuracy of the experiment, is equal to the sphere diameter. This implies that the spheres are close packed, with a volume fraction of $\phi\approx0.74$ in the crystals. Since this is substantially larger than the average volume fraction of the sample, there are presumably some regions of the cell with a decreased volume fraction. Alternatively, it is perhaps possible that the spheres are close packed within the hcp planes, but the planes are not touching each other, but are separated by a larger spacing. However, this seems unlikely as we would expect the nonuniform separation of the spheres to relax after the shear ceases. Thus the origin of this observation must lie in some other nonuniformity of the packing.

To investigate the origin of this behavior, we placed the screen for the observation of the diffraction directly against the back surface of the cell. In this case, the distances between the screen and the two faces of the cell are comparable. We observe a dramatically different pattern. Instead of six diffraction spots, we see 12 spots, arranged in two distinct sets of six. One set is closer to the incident beam than the other. The variation in the spacing is not due to different lattice constants within the crystal. Instead, this pattern is due to diffraction from two different crystals, one near each face of the cell. Since the screen is so close to the diffracting crystals, we are able to distinguish between the crystals that cause each of them. The set with the narrow spacing arises from a crystal near the wall closer to the screen, while the set with the wide spacing arises from a different crystal, near the wall farther from the screen. This accounts for the observation of an increased value of ϕ: The shear-aligned crystals form only on the two faces of the cell, while the colloid in the middle of the cell remains a fluid. The volume fraction of the crystalline region is then higher than that of the fluid, implying that the shear-aligned crystals are more nearly close packed. The preferential formation of crystals nearer to the cell walls as compared to the middle of the cell is consistent with the amplitude of the shear across the thickness of the cell. The local flow pattern is Poiseuille flow, which has zero velocity at the two walls, a maximum velocity in the center of the cell, and a parabolic velocity profile in between. Thus the shear is a maximum nearest the two walls, and decreases to zero towards the center of the cell. The crystals will be preferentially shear aligned near the walls of the cell, where the shear is largest. To verify that the crystals are formed only near the cell walls, we observed the scattering from the cell with a focused laser beam incident on the narrow side. While it was not possible to measure the diffraction pattern, it was possible to determine whether or not there were Bragg reflections as the focused spot was scanned across the width of the cell. Bragg reflections were observed only for the roughly one-third of the sample near each wall, and were not observed for the middle third of the sample. This confirms our observation that the crystal is formed only in the regions of high shear near the cell walls.

While the diffraction pattern from the lower half of the cell consists of two distinct sets of six spots each, the pattern from the upper half of the cell is markedly different. It also consists of two distinct sets of diffraction spots from crystals near each face of the cell. However, each set consists of not six, but only three diffraction spots, with threefold symmetry, as shown in Fig. 3. The orientation of one set is rotated by 180° with respect to the other. In the far field, these two sets of spots appear as a sixfold symmetric pattern similar to that observed from the lower half of the cell. It is only when observed with the screen very close to the cell that this new diffraction pattern is observed and the different spacings of the two patterns can be distinguished.

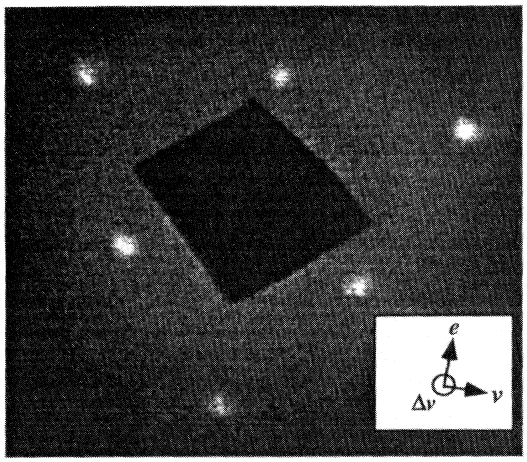

FIG. 3. Diffraction pattern from the shear-aligned colloidal crystal, showing two sets of three Bragg peaks, one with wider spacing, resulting from a crystal near the cell wall farther from the screen, and the second with narrower spacing, resulting from a crystal near the cell wall closer to the screen. The patterns are rotated by 180° with respect to one another, and arise from two different, but nearly perfect, fcc twins. The inset indicates the directions of velocity v, shear Δv, and vorticity e.

The regions with threefold symmetry are not observed everywhere in the upper half of the cell. Some areas have crystals with diffraction patterns exhibiting sixfold symmetry similar to the crystals in the bottom half of the cell. Other areas possess crystals which exhibit three intense diffraction spots and three weaker diffraction spots rotated by 180° from the intense spots. However, most of the upper half of the cell is comprised of crystals which exhibit the threefold symmetric diffraction pattern and no intensity is observed in the positions where the other three spots would occur if the pattern were sixfold symmetric. To verify this, diffraction images exhibiting the threefold symmetric pattern, such as the one shown in Fig. 3, were digitized and the intensities were measured more quantitatively. We find that the intense set of diffraction spots is always at least a factor of 10 more intense than background scattering in the vicinity of the missing spots. This background, which we believe is due to the scattering from the liquid portion of the sample in the middle of the cell, sets the lower limit of our detection of the weaker diffraction spots.

The structure and orientation of the crystals whose diffraction pattern is shown in Fig. 3 is quite surprising. The orientation of the pattern implies that a line of close-packed spheres, in the **a** direction, is aligned along the final velocity direction. The choice of a particular twin depends on the translation of each successive layer in a direction perpendicular to the velocity, in the direction of the vorticity **e**, as shown in the inset in Fig. 3. A hard-sphere system does not possess any long-range interactions, which are normally required to achieve a perfect fcc or hcp structure. Instead, a hard-sphere colloidal crystal is normally comprised of a random stacking of the three orientations of the planes [14], as observed towards the bottom of the cell. Shear will align the planes with the **a** direction parallel to the velocity, but the stacking of the planes remains random [6,7]. A fcc structure has been observed for steady shear rates of less than 1 sec^{-1}, for suspensions with the same volume fractions. Oscillatory shear with strains on the order of unity also leads to fcc structures with temporally alternating twins. However, in both cases, the fcc structures are oriented with the **a** direction *normal* to the velocity, and thus are rotated by 90° with respect to the structures observed here. Perfect fcc crystals, with the twin determined by the vorticity direction, have not previously been observed for shear-aligned, hard-sphere colloids.

We believe that this surprising structure results from the way the shear is applied to our samples. The macroscopic flow of the suspension as the cell is rocked results in a small additional variation of the velocity, and an increased strain, normal to the shear provided by the Poiseuille flow, as shown in Fig. 1. This additional strain may force further ordering in the stacking, making one twin dominant. The dominant shear normal to the walls would cause the hcp layers to align parallel to the wall surface. The additional shear would give each successive row of particles closer to the top within the layer a slightly greater velocity. This may cause the particles to preferentially stack in a single twin of the fcc structure. This would account for the prevalence of the fcc structures in the upper half of the cell, where the macroscopic flow is more extensive than the lower half. Moreover, it would also account for the formation of the opposite twins on either side of the cell.

COHERENCE EFFECTS

The shear-aligned fcc crystals produced by these hard-sphere colloids are quite unusual. They are highly ordered as the three diffraction spots are quite sharp. Moreover, the crystals consist of only a single twin of the two possible fcc structures, as no intensity due to the second twin is observed. However, the same diffraction pattern is again observed with all laser lines. Thus the crystal cannot be a pure fcc structure, but must have sufficient defects to broaden the diffraction along q_l in order for it to be observed with all laser lines. These defects are presumably again introduced by stacking faults in the packing of the hcp planes. These must lead either to local regions of hcp packing or local regions of the other twin of the fcc structure. However, each of these structures would result in a sixfold symmetric diffraction pattern, so that the number of these defects must be sufficiently small as not to lead to any intensity in the other three diffraction spots. Moreover, after any stacking fault, the structure must revert back to the packing of the dominant twin. This form of packing seems unique to shear-aligned crystals made of hard-sphere colloids.

Further proof of the existence of defects on the crystal structure comes from a closer examination of the diffraction spots. The intensity in these spots is not uniform, but is instead made up of a random speckle pattern, as shown in Fig. 4(a). A speckle pattern is very generally observed when the illuminating source is coherent, and when the scattering object produces scattering with ran-

dom phase [19]. Speckle patterns in Bragg peaks are extremely difficult to observe in x-ray crystallography because of the lack of the required coherence in the source. However, they can be observed by exploiting the very high brightness of modern synchrotrons which enable the required spatially coherent beam to be attained [13].

The diffraction spot shown in Fig. 4(a) is obtained with a weakly focused incident laser beam, with a spot size of roughly 500 μm. There are speckle spots in both directions of the image. This implies that there are defects in the packing of the crystal within each hcp plane as well as in the stacking of the planes themselves. However, by focusing the laser beam more tightly, we can reduce the area of each hcp plane that is illuminated, and ensure that a speckle spot from each plane is larger than the diffraction spot. However, we cannot reduce the size of the speckle spot due to the thickness of the crystal. When the beam is focused to a spot of roughly 40 μm in diameter, the diffraction spot changes its appearance dramatically, as shown in Fig. 4(b). In this case, the speckle pattern is no longer a two-dimensional pattern of spots, but instead fluctuates in only one dimension. The orientation of these spots is always in the same direction. The long axis of the spots is always perpendicular to the direction of incident laser beam, and is the same for all the spots. The intensity always fluctuates in a direction leading radially out from the laser beam. To clarify the origin of this speckle pattern, we illustrate the scattering geometry for one of the Bragg spots in Fig. 5. Here we show a rod which represents the intensity in reciprocal space along q_l corresponding to the broadening of the reciprocal lattice points because of the stacking defects. The overall intensity distribution along this rod is determined by the nature of the stacking defects. However, for a single realization of the crystal and a coherent source, the intensity fluctuates rapidly, as shown on the right of the rod. The Ewald sphere, defined by the incident and diffracted beams, intersects a portion of this rod. The rod is broadened in the h and k directions because of the finite size of the illuminated region of the crystal. The Ewald sphere cuts this broadened rod at an angle, probing the intensity along this cut. If the intensity varies only along the q_l direction, the projection of this variation onto the Ewald sphere will result in a speckle pattern in only one direction, which will always be perpendicular to the incident laser beam, for all the Bragg spots. This is exactly what is observed with a focused laser beam. Since the variation of the intensity is restrict-

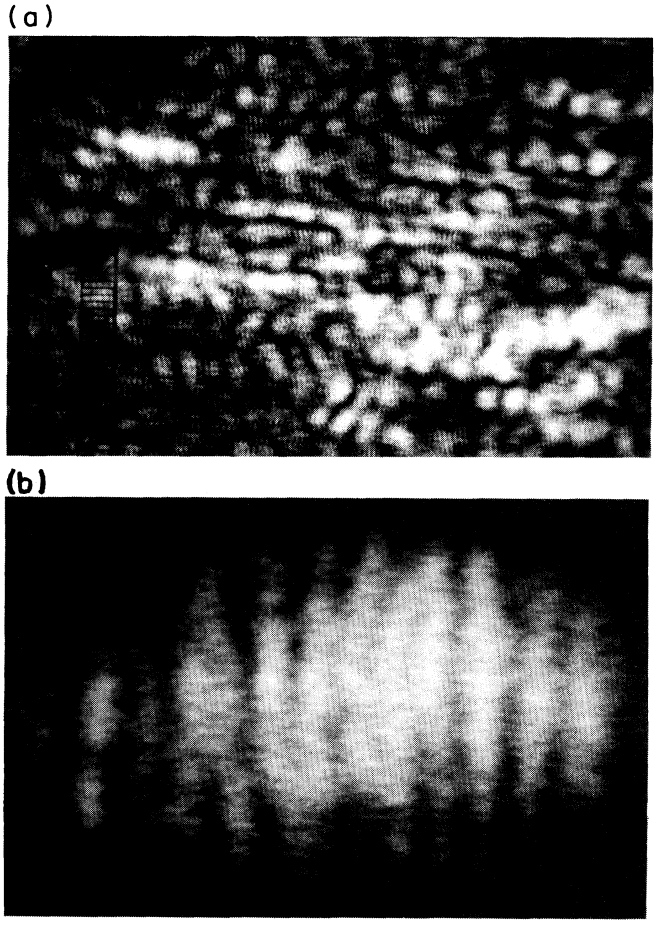

FIG. 4. (a) Closeup photograph of a single Bragg diffraction spot when the laser beam has a diameter of about 500 μm, showing the specklelike intensity fluctuations in both directions. (b) Closeup photograph of a single Bragg diffraction spot when the laser beam has a diameter of about 40 μm, showing the specklelike intensity fluctuations only in the q_l direction. When this speckle pattern is observed, the fluctuating direction is always perpendicular to the incident laser beam. Both photographs are oriented so that the horizontal direction is perpendicular to the incident laser beam, corresponding to the direction along q_l. The very-small-scale fluctuations visible on the photographs result from interference between the two surfaces of the cell.

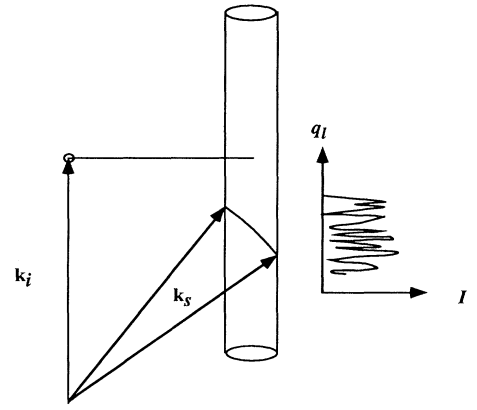

FIG. 5. Schematic view of a portion of the Ewald sphere which determines the Bragg peak. The intensity of the peak is broadened in the two directions normal to the incident beam, along **h** and **k**, due to the finite size of the crystal that is illuminated. The Ewald sphere interesects a portion of the intensity of the rod along q_l. Stacking defects broaden the Bragg peak in the q_l direction, and result in the fluctuations of the intensity in a single direction. Fluctuations in the intensity of the Bragg peak are observed in only one direction, and can be caused only by the packing defects, which result in the fluctuations along q_l. These fluctuations are illustrated schematically on the right of the diagram.

ed to the q_l direction, it can only be caused by stacking faults, not by packing defects within the hcp planes. By contrast, observation of speckle in both directions implies that the rod has intensity variations in both the **h** and the **k** directions, as well as, possibly, the l direction. Thus this pattern must also reflect packing defects within the hcp planes themselves.

The pattern observed with the focused beam confirms the existence of the stacking defects. It allows us to focus on the nature of these defects. The angular width of the speckle spots is directly related to the thickness of the crystal, providing an ideal method for determining the amount of the sample that has been formed into shear-aligned crystal. From the angular width of the speckle spots, we find that crystal on each side of the cell has a thickness of between $\frac{1}{4}$ and $\frac{1}{3}$ of the cell. This is consistent with our measurement of the presence of diffraction using a laser beam focused onto the thin side of the cell.

To obtain a clearer understanding of the structure and its coherent crystallography, we perform a computer calculation of the diffraction pattern, similar to that done for atomic systems [12]. To ensure that speckle is observed, we calculate the diffraction from a *single* realization of a fcc crystal containing stacking defects. For each value of q, we sum the fields, using the form factor for a hcp plane, and square the total to obtain the intensity. We calculate the intensity along the q_l direction for the $hkl=\{10l\}$ and $\{01l\}$ rods, which are each representative of a set of three equivalent rods, thereby allowing us to determine the symmetry of the diffraction pattern [18]. For a single twin of a perfect fcc crystal, an intensity maximum would be observed at $q_l=2\pi/3d_l$ for one of these rods, and at $q_l=4\pi/3d_l$ for the second rod, where d_l is the interlayer spacing. We begin with a perfect *ABCABC* stacking of a single fcc twin. We introduce random defects in the packing of the structure with a probability α, but force the structure to revert back to the same *ABCABC* structure after the defect. This scheme allows us to tune the structure from one twin to the other, while ensuring that we have predominantly a single twin, and hence a threefold symmetric diffraction pattern, even as we introduce more defects by varying the value of α. We note that this model is very different from that used by Pusey *et al.* [14], where α was used to tune the structure between hcp and fcc stacking. Their model would not describe the structures we observe for shear-aligned fcc crystals. Moreover, their model did not explicitly consider speckle in the scattering.

We perform the calculation for a stacking of 550 hcp planes, which we estimate to be the number of planes in a crystal whose width is $\frac{1}{3}$ the thickness of the cell. For $\alpha<0.1$, there are so few defects in the stacking that the widths of the diffraction peaks along q_l are too narrow to allow simultaneous observation with all laser lines. As α is increased to 0.1, there are sufficient defects to broaden the diffraction peaks enough to be observable with all laser lines. Furthermore, the observed pattern still possesses threefold symmetry, in that the three stronger spots are at least a factor of 35 more intense than the three weaker spots. This ratio decreases to 10 for $\alpha=0.2$. By the time $\alpha=0.3$, the pattern consists of three strong spots and three weak spots, while for $\alpha=0.5$, the pattern exhibits sixfold symmetry, corresponding to a random stacking of hcp planes.

For all values $0<\alpha<1$, we observe speckle in the diffraction pattern along q_l reflecting the randomness in the stacking. The width of the speckle along q_l varies inversely with the thickness of the crystal, as expected. We compare a calculated speckle pattern with the measured intensity in Fig. 6. The calculated intensity, Fig. 6(b), is obtained for a single realization of a crystal of 550 planes, using $\alpha=0.2$. The measured intensity, Fig. 6(a), is obtained by digitizing an image of a diffraction spot and taking a cut of the intensity along q_l. We do not expect perfect correspondence, since the calculation and data reflect different single realizations of the random stacking. However, we do expect the observed pattern to appear qualitatively similar to the calculated pattern. Both exhibit the same features of random fluctuations, with the same overall characteristics, as expected.

The spacing of the speckle in the calculated pattern is nearly identical to that in the measured pattern. This confirms that the crystal thickness is about $\frac{1}{3}$ of the cell thickness. In fact, the speckle provides the best measure of the thickness, as the width of the diffraction peak along q_l is difficult to determine. Also shown in Fig. 6(c) is the intensity calculated over a larger range of q_l for $\alpha=0.2$. This demonstrates the overall speckle pattern, and illustrates the broadening of the diffraction peak due to the stacking disorder. Using this model to describe the

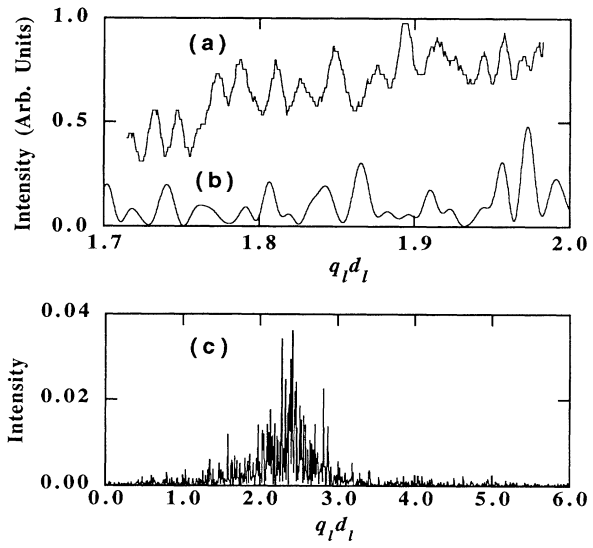

FIG. 6. Comparison of the diffracted intensity as a function of q_l for (a) the experimental measurement and (b) the calculation. Each represents the intensity from a single realization of the crystal, and exhibits similar, but not identical, fluctuations. Also shown is (c) the calculated intensity over a wider range of q_l, showing the speckle pattern and the broadening of the diffraction peak due to the stacking disorder. The broadening is sufficient to allow observation of the Bragg peaks at all laser wavelengths, but still maintain the observed threefold symmetry. The calculations are performed with a value of $\alpha=0.2$.

disorder, we are able to determine the value of α required to adequately describe the data. The Bragg peak must be sufficiently broadened along q_l to allow Bragg spots to be observed by all laser lines. However, the broadening must not be so large as to induce sixfold symmetry instead of the observed threefold symmetry. These constraints allow us to determine that, within this model, α must lie between 0.1 and 0.2.

CONCLUSIONS

We have presented the results of a study of the structure of suspensions of hard-sphere colloids that are shear aligned by rocking the thin cuvette in which the colloids are contained. The dominant shear results from the Poiseuille flow across the thin wall of the cell, and this aligns the sample into ordered crystals. However, since the shear reaches a maximum near the two walls of the cell, the crystals are formed only near the walls in the regions of maximum shear. The sample in the middle third of the cell remains a fluid. The index of refraction of the particles is matched to that of the suspending fluid, eliminating any multiple scattering of light and allowing the structure of the shear-aligned colloidal crystals to be determined by laser crystallography. The spacing of the spheres in the crystals is determined from the diffraction pattern and suggests that the volume fraction of the crystals is nearly close packed, $\phi \approx 0.74$. This suggests that the fluid in the center of the cell has a lower volume fraction, in order to maintain the total volume fraction at the initial value of $\phi \approx 0.56$. The structure of the crystals in the lower half of the cell is predominantly randomly stacked layers of hcp planes, with these planes lined along the walls of the cell. The structure of the crystals in the upper half of the cell is predominantly fcc, as evidenced by the threefold symmetric diffraction pattern. Moreover, the crystals on each side of the cell consist of nearly perfect fcc twins, with opposing twins on either side of the cell. We believe that this structure results from the additional shear imposed by the macroscopic flow of the sample as it is rocked, which preferentially packs the spheres into single fcc twins.

Although we observe a single twin of a fcc crystal, the structure cannot be perfect, as we observe the same diffraction pattern with all the laser wavelengths used. To describe the data, we use a simple model of the structure consisting of a fcc stacking of hcp planes. We introduce stacking defects with a probability α, but insist that the original fcc stacking is recovered immediately after the defect. This is required to ensure that the threefold symmetry of a single twin of fcc crystal is observed. This model maintains the observed threefold symmetry, while also allowing the Bragg peaks to be sufficiently broadened to be observable with all laser lines. Good agreement is found between the model and the data for values of α between 0.1 and 0.2.

We also observe a speckle pattern within the Bragg peaks themselves. This speckle pattern is observable because a coherent laser source is used to perform the crystallography. When the laser beam is only weakly focused, a two-dimensional speckle pattern is observed within the Bragg peaks. By contrast, when the laser beam is focused to a sufficiently small spot size, specklelike fluctuations are observed in only one direction. This must reflect disorder in only one direction, and from the orientation of the speckle fluctuations, this is determined to be the stacking direction. Thus the speckle reflects the defects in the stacking of the hcp planes as they are aligned by the shear. The observation of this speckle pattern confirms the existence of these defects. Moreover, this observation confirms a recent theoretical prediction [12] of speckle on the Bragg peaks resulting from this form of packing disorder. The prediction was originally made for atomic crystals, but the speckle in these would be very difficult to observe because of the lack of coherence in x-ray sources used for crystallography.

These speckle fluctuations in the Bragg peaks reflect the stacking disorder of the structure, and monitoring their temporal changes could provide rich information about the dynamics of the shear alignment. In addition, the type of shear used here might allow the formation of very highly ordered and aligned single crystals of colloids. These structures may potentially have a wide range of uses.

ACKNOWLEDGMENTS

We thank Dov Levine, Peter Pusey, and Tom Witten for helpful discussions, Peter Pusey for the colloids, and DOE Contract No. DE-FG05-88ER45349 for support of B.J.A.

[1] P. N. Pusey and W. van Megan, Nature (London) **320**, 340 (1986).
[2] P. N. Pusey and W. van Megan, Phys. Rev. Lett. **59**, 2083 (1987).
[3] R. L. Hoffman, Trans. Soc. Rheol. **16**, 155 (1972).
[4] R. L. Hoffman, J. Colloid Interface Sci. **46**, 491 (1974).
[5] G. N. Choi and I. M. Kreiger, J. Colloid Interface Sci. **113**, 101 (1986).
[6] B. J. Ackerson and P. N. Pusey, Phys. Rev. Lett. **61**, 1033 (1988).
[7] B. J. Ackerson, J. Rheol. **34**, 553 (1990).
[8] N. J. Wagner and W. B. Russel, Physica A **475**, 155 (1989).
[9] S. E. Paulin, B. J. Ackerson, and M. S. Wolfe, in *Complex Fluids,* edited by E. B. Sirota, D. A. Weitz, T. A. Witten, and J. Israelachvilis, MRS Symposia Proceedings No. 248 (Materials Research Society, Pittsburgh, 1992) p. 259.
[10] H. K. Bowen, Mater. Sci. Eng. **44**, 1 (1980).
[11] J. Martorell and N. M. Lawandy, Phys. Rev. Lett. **66**, 887 (1991).
[12] A. Garg and D. Levine, Phys. Rev. Lett. **60**, 2160 (1988).
[13] M. Sutton, S. G. J. Mochrie, T. Greytak, S. E. Nagler, L. E. Berman, G. A. Held, and G. B. Stephenson, Nature (London) **352**, 608 (1991).
[14] P. N. Pusey, W. van Megan, P. Bartlett, B. J. Ackerson, J. G. Rarity, and S. M. Underwood, Phys. Rev. Lett. **63**, 2753 (1989).

[15] S. E. Paulin and B. J. Ackerson, Phys. Rev. Lett. **64**, 2663 (1990).
[16] S. Hendricks and E. Teller, J. Phys. Chem. **10**, 147 (1942).
[17] A. J. C. Wilson, Proc. R. Soc. London, Ser. A **180**, 277 (1942).
[18] A. Guinier, *X-Ray Diffraction* (Freeman, New York, 1963).
[19] J. C. Dainty, *Laser Speckle and Related Phenomena* (Springer-Verlag, New York, 1984).

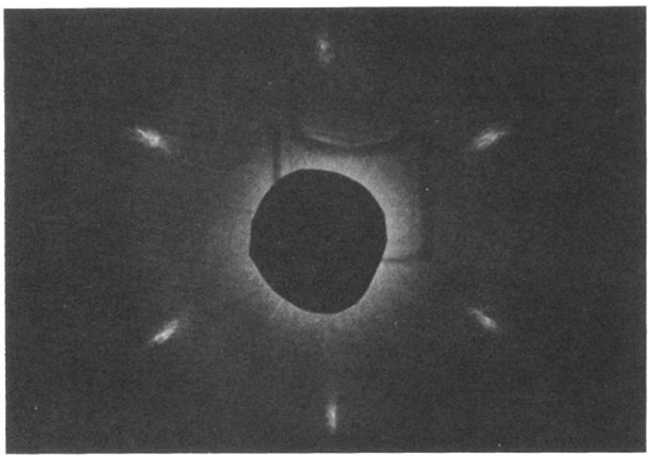

FIG. 2. Diffraction pattern of a shear-aligned colloidal crystal, showing six sharp Bragg peaks. The laser beam is incident near the bottom of the cell.

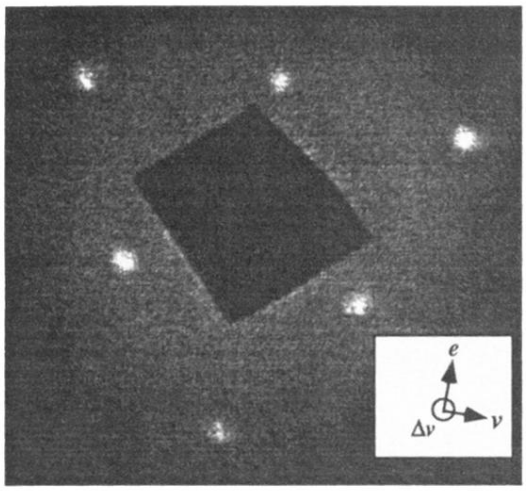

FIG. 3. Diffraction pattern from the shear-aligned colloidal crystal, showing two sets of three Bragg peaks, one with wider spacing, resulting from a crystal near the cell wall farther from the screen, and the second with narrower spacing, resulting from a crystal near the cell wall closer to the screen. The patterns are rotated by 180° with respect to one another, and arise from two different, but nearly perfect, fcc twins. The inset indicates the directions of velocity v, shear Δv, and vorticity e.

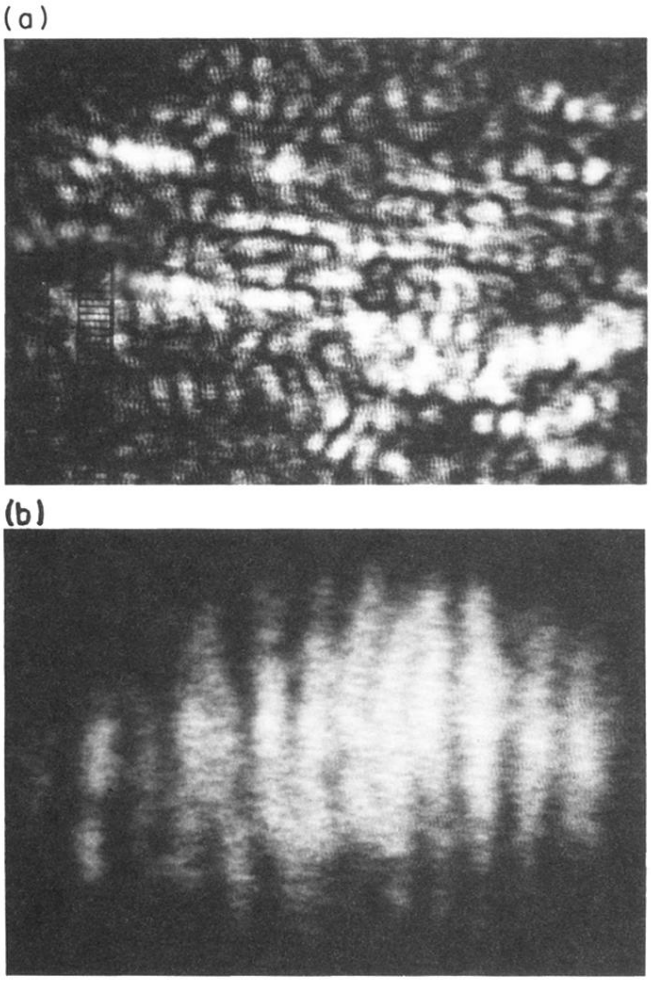

FIG. 4. (a) Closeup photograph of a single Bragg diffraction spot when the laser beam has a diameter of about 500 μm, showing the specklelike intensity fluctuations in both directions. (b) Closeup photograph of a single Bragg diffraction spot when the laser beam has a diameter of about 40 μm, showing the specklelike intensity fluctuations only in the q_l direction. When this speckle pattern is observed, the fluctuating direction is always perpendicular to the incident laser beam. Both photographs are oriented so that the horizontal direction is perpendicular to the incident laser beam, corresponding to the direction along q_l. The very-small-scale fluctuations visible on the photographs result from interference between the two surfaces of the cell.